Met. Mater. Int., Vol. 20, No. 6 (2014), pp. 1085~1093
doi: 10.1007/s12540-014-6012-8

Effect of Boundary Conditions on the Numerical Solutions of Representative Volume Element Problems for Random Heterogeneous Composite Microstructures

Yi Je Cho[1], Wook Jin Lee[2], and Yong Ho Park[1,*]

[1]Pusan National University, Department of Materials Science and Engineering, Busan 609-735, Korea
[2]Empa Swiss Federal Laboratories for Materials Science and Technology, CH-8600 Dübendorf, Switzerland

(received date: 28 December 2013 / accepted date: 7 April 2014)

Aspects of numerical results from computational experiments on representative volume element (RVE) problems using finite element analyses are discussed. Two different boundary conditions (BCs) are examined and compared numerically for volume elements with different sizes, where tests have been performed on the uniaxial tensile deformation of random particle reinforced composites. Structural heterogeneities near model boundaries such as the free-edges of particle/matrix interfaces significantly influenced the overall numerical solutions, producing force and displacement fluctuations along the boundaries. Interestingly, this effect was shown to be limited to surface regions within a certain distance of the boundaries, while the interior of the model showed almost identical strain fields regardless of the applied BCs. Also, the thickness of the BC-affected regions remained constant with varying volume element sizes in the models. When the volume element size was large enough compared to the thickness of the BC-affected regions, the structural response of most of the model was found to be almost independent of the applied BC such that the apparent properties converged to the effective properties. Finally, the mechanism that leads a RVE model for random heterogeneous materials to be representative is discussed in terms of the size of the volume element and the thickness of the BC-affected region.

Keywords: computer simulation, representative volume element, boundary conditions, heterogeneous materials, micromechanics

1. INTRODUCTION

The homogenization of randomly microstructured heterogeneous materials has been a subject of continuing interest for many years, since most engineering materials have random and heterogeneous microstructures in nature (e.g. polycrystalline alloys, dual- or multi-phase alloys, porous materials, composites, etc.). Textured metal materials such as hot-rolled steel have crystallographic and morphological orientations, but still have randomness and non-repeatability in their microstructures. For this purpose, a wide variety of semi-analytical and numerical methods have been developed in the literature. In this regard, the development of representative volume element (RVE) approaches, in conjunction with numerical methods such as the finite element method (FEM), has enabled the prediction of the full 3D mechanical response of heterogeneous materials undergoing motion or deformation [1-4]. This approach has been well documented for studying the response of randomly distributed filaments [5,6], spherical inclusions at the microscale [7-9], porous microstructure [4], and the crystal plasticity model for polycrystalline [2] or dual-phase steel on fracture toughness [10] and void formation [11].

In the literature, several definitions of a RVE have been proposed for different purposes. According to Hill [12], the RVE should be a volume of heterogeneous material that is sufficiently large to be statistically representative, ensuring a sample is taken of all microstructural heterogeneities that occur in the composite. He stated that the apparent overall moduli of the RVEs should be independent of the surface values of traction and displacement, as long as these values are macroscopically uniform. This definition proposed by Hill was later extended by Hashin [13]. He suggested that the RVE should be large enough to contain sufficient information on the microstructure in order to be representative; however, it should be much smaller than the macroscopic body (This is commonly known as the Micro-Meso-Macro principle). Another definition of the RVE was recently proposed by Drugan and Willis [14]. They asserted that the RVE should contain the smallest volume of material to define the macroscopic structure, but

*Corresponding author: yhpark@pusan.ac.kr

the volume should be large enough to remain constitutively valid. Kanit *et al.* [3] later proposed the definition that the RVE be regarded as a volume V sufficiently large to be statistically representative of the material. This is derived from the knowledge of the statistical nature of the microstructure in order to characterize the macroscopic constitutive response of a heterogeneous material. They also stated the definition based on statistical properties that the RVE must ensure a given accuracy of the overall estimated properties obtained by spatial averaging of the stress, the strain, or the energy fields.

For practical use, one of the most important points in the RVE approach is the determination of the appropriate size of the volume elements of heterogeneous materials to be computed in order to get a precise enough estimate of effective properties. As the size of the RVE increases, it is appropriate to present the deformation behaviors of real microstructure as long as a sufficient number of microstructural factors are considered. However, in practice computational costs usually limit the possible number of microstructural factors (e.g. number of inclusions, grains, pores, etc.) that can be handled in the simulation of one volume element V, whose limited volume is generally less than the RVE of the material [3]. In this case, the properties that can be computed are not necessarily the desired effective properties, but merely the apparent properties of the investigated volume. It is known that the RVE is morphology and property dependent, so that a well-suited parameter is necessary for quantitative comparisons. Such a parameter has been proposed by Kanit *et al.* [3] and Gitman *et al.* [7], and utilized for many RVE studies [6,8,10,15-17].

When estimating the mechanical or physical properties of heterogeneous materials using RVEs, another important point to consider is the choice of appropriate BCs, since the apparent properties of the volume element are influenced by the type of BCs used in the simulations. In RVE approaches, several types of BCs can be prescribed on V to impose a given mean strain or mean stress on the material element. As stated by Sab [18] and Kanit [3], the response of the RVE must be independent of the type of BCs. In Refs. [19,20], Huet derived relationships between the apparent physical properties obtained from a large microstructure and from a set of smaller ones resulting from the uniform partitioning of the original sample. He considered three different BCs for his study: the first was the kinematic uniform boundary condition (KUBC), the second was the static uniform boundary condition (SUBC) and the third was the orthogonal mixed boundary condition (OMBC). One of the main conclusions drawn from these studies was that the effective properties were bounded by the ensemble average of the results obtained on the set of smaller specimens. The effective properties were shown to always fall between the apparent properties associated with the SUBC and KUBC. He also showed that when a large specimen (or microstructure) is considered as RVE, the apparent properties found with both SUBC and KUBC are almost identical and therefore were almost equal to the effective properties of the material. These conditions will be discussed in more detail in Section 2.2 of the paper.

Although a lot of research has focused on determining the proper size and representativity of RVEs, the mechanical origin of the discrepancy between the apparent properties obtained with different BCs and with the effective properties is not yet clearly established in the literature. Since the accuracy and representativity of RVEs are strongly related to the discrepancies between the solutions obtained with different BCs, more fundamental research on these discrepancies would be worthwhile to quantify the representativity of RVE models for better understanding and exploitation. The study presented in this paper aimed at researching this phenomenon, namely the different mechanical responses of RVEs associated with different types of BCs and with different volume element sizes. Numerical investigations were carried out to simulate the uniaxial tensile deformations of elastic, dual-phase random heterogeneous microstructures with two different BCs. Comparisons of the strain fields which were induced by the two different boundary conditions allowed a mechanical scenario to be established describing how the specific volume element of random microstructures could be representative of the whole structure, and could be used to estimate its effective properties.

2. NUMERICAL PROCEDURE

2.1. Model geometry, finite element meshes and materials properties

A good example to study the general aspect of simulating random heterogeneous media behaviors is probably the spherical particle reinforced composite model, since it has a relatively simple, dual-phase microstructure within which the particle distribution is random [8,9]. In this paper, testing was conducted on a composite material with spherical reinforcing phases. Because the main purpose of this paper was to investigate the effect of different types of BCs on the mechanical responses of RVE models, simple plane stress was considered using a 2D model of the microstructure of the composite.

The 2D volume elements for the random particle reinforced composite were produced by a random sequential adsorption (RSA) algorithm [21]. The RSA algorithm used for the generation of the volume elements involved adding spherical particles sequentially to square areas by randomly generating the center point of each particle. During the RSA procedure, newly generated candidate particles were deleted if they overlapped with any particles that had been generated previously. The minimum distance between each particle was set to one tenth of the radius of the particles, which was imposed by the practical limitations of creating an adequate finite element mesh in the matrix between particles. Further details as

well as the flow chart of this procedure can be found in the authors' previous publications [22,23]. The RSA algorithm in combination with the above conditions was used to generate the volume elements of the composite microstructure. The diameter of the reinforcing particles was chosen to be 1 mm.

The constitutive equations adopted for modeling the response of the phases were based on a simple standard linear elastic framework. Thus the material properties of each phase were defined by two parameters: Young's modulus (E) and Poisson's ratio (ν). These material parameters are given in Table 1. As shown in Table 1, the elastic modulus of the particles was set higher than that of the matrix, as is the case for ceramic particle reinforced aluminum matrix composites. All of the finite element calculations were performed with the commercial ANSYS software [24].

Table 1. Mechanical properties of the reinforcement particles and the matrix material used for the simulations

Material	Elastic modulus (E/GPa)	Poisson's ratio (υ)
Matrix	68	0.36
Particle	470	0.17

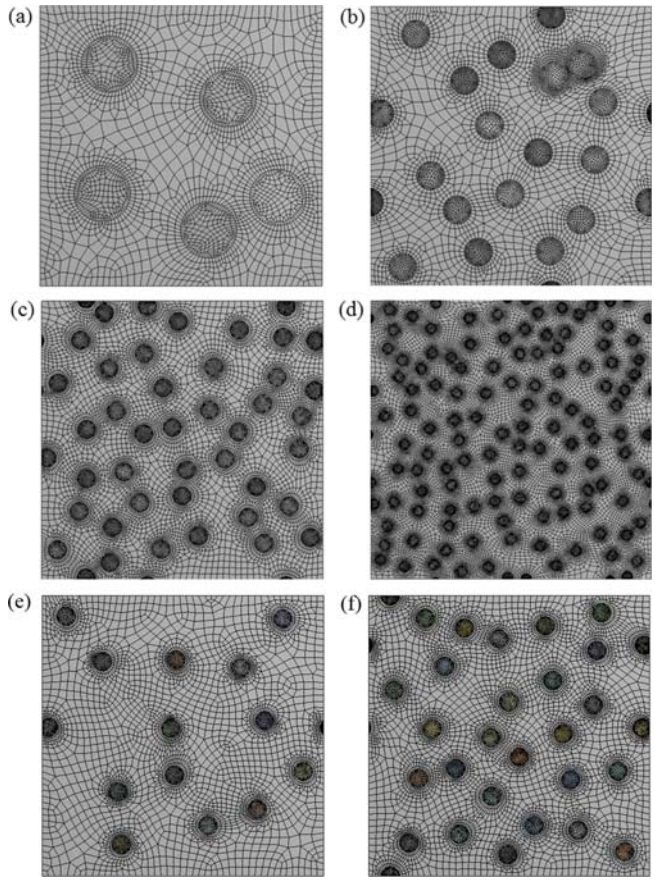

Fig. 1. Model geometries and meshes of volume element models with different sizes. (a) 5×5 mm^2, (b) 10×10 mm^2, (c) 15×15 mm^2, (d) 25×25 mm^2, and (e, f) 15×15 mm^2 with 5 and 10% particle volume fractions, respectively.

In order to address the effect of volume element size in RVE modeling, several different square volume elements with side lengths L of 5, 10, 15, and 25 mm were generated using the RSA algorithm. Figures 1(a)-(d) show the typical geometries and finite element meshes of the volume elements with a particle volume fraction of 15% for different sizes of the models. To investigate the effect of the volume fraction of the particles, two additional models with volume fractions of 5 and 10% were also reconstructed using the same algorithm, with a fixed side length of 15 mm (Figs. 1(e) and (f)). The models were meshed with four-node quadrilateral elements using the automatic meshing algorithm provided by ANSYS. The meshes were made finer near the particle/matrix interfaces, and the mesh densities for each volume element model were set similar to one another to avoid any mesh density related errors in comparative studies.

2.2. Boundary conditions

According to previous work by Hill [12], the necessary and sufficient conditions for equivalence between the energetically and mechanically defined properties of elastic materials are contained in the Hill condition:

$$\langle \boldsymbol{\sigma} : \boldsymbol{\varepsilon} \rangle = \langle \boldsymbol{\sigma} \rangle : \langle \boldsymbol{\varepsilon} \rangle \tag{1}$$

where $\boldsymbol{\sigma}$ and ε are the stress and strain tensors, respectively. The bracket '$\langle\ \rangle$' means a volume average of the variable. This condition means that the average of the product of the stress and strain tensors at a lower (micro) level equals the product of their averages at a higher (macro) level. Using Gauss' theorem, the above condition can be generalized to heterogeneous materials as [25]:

$$\int_{\Gamma} (\boldsymbol{t}(\boldsymbol{x}) - \langle \boldsymbol{\sigma} \rangle \boldsymbol{n}) \cdot (\boldsymbol{u}(\boldsymbol{x}) - \langle \boldsymbol{\varepsilon} \rangle \boldsymbol{x}) d\Gamma \tag{2}$$

where Γ is the boundary of a volume element V and $\boldsymbol{t}$, $\boldsymbol{u}$, $\boldsymbol{n}$, $\boldsymbol{x}$ are the traction, displacement, normal, and position vectors, respectively. As stated by Hazanov and Amieur [26] and Ostoja-Starzewski [15], this condition requires that the body be loaded in a specific way on its boundary Γ to form a finite heterogeneous body. Furthermore, considering the decomposition of the displacement vector into a homogeneous deformation $\bar{\boldsymbol{u}}$ and a fluctuation field $\tilde{\boldsymbol{u}}$ along the boundaries of V, the following conditions must be satisfied:

$$\boldsymbol{u} = \bar{\boldsymbol{u}} + \tilde{\boldsymbol{u}} \tag{3}$$

$$\frac{1}{V} \int_{\Gamma} (\tilde{\boldsymbol{u}} \otimes \boldsymbol{n} + \boldsymbol{n} \otimes \tilde{\boldsymbol{u}}) dA \tag{4}$$

for a boundary area A and with $\boldsymbol{n}$ the outward normal vector to Γ. It is then possible to classify the type of boundary conditions in terms of their fluctuating part. A typical classification with descending restrictiveness for satisfying this

condition (on boundary Γ) is as follows:

1. KUBC: the displacement $\boldsymbol{u}$ along the entire boundary of V is homogeneous, i.e. no boundary strain fluctuations are feasible.

$$\tilde{\boldsymbol{u}} = 0, \boldsymbol{u}(\boldsymbol{x}) = \boldsymbol{\varepsilon} \tag{5}$$

2. Static uniform (SUBC) or traction control boundary condition: the traction vector $\boldsymbol{t}$ at the boundary of V is given by:

$$\boldsymbol{t}(\boldsymbol{x}) = \boldsymbol{\sigma}\boldsymbol{n} \tag{6}$$

3. Orthogonal mixed (OMBC) or uniform displacement-traction condition:

$$(\boldsymbol{t}(\boldsymbol{x}) - \boldsymbol{\sigma}\boldsymbol{n}) \cdot (\boldsymbol{u}(\boldsymbol{x}) - \boldsymbol{\varepsilon}\boldsymbol{x}) = 0, \tilde{\boldsymbol{u}} = 0 \tag{7}$$

4. Periodic boundary condition (PBC): The fluctuation field has the same value on opposing points of the volume element. For any opposing points x_1^+ and x_1^-, the fluctuation strain has to satisfy

$$\tilde{u}(x_1^+) = \tilde{u}(x_1^-) \tag{8}$$

where, $\boldsymbol{\varepsilon}$ and $\boldsymbol{\sigma}$ denote macroscopically prescribed constant tensors.

With the OMBC, different combinations of the prescribed boundary vectors are possible but have to fulfill the Eq. 7. For uniaxial tensile or compressive deformation analysis using the OMBC, uniaxial displacement along one direction of V with free lateral boundaries has been frequently used in the literature (e.g. [20,27,28]). In general, the apparent moduli obtained with the KUBC and SUBC can respectively be thought of as upper and lower bounds for the effective moduli, and the ones obtained with the OMBC and PBC usually lie in between these bounds. With increasing volume element V, the moduli obtained with the KUBC and SUBC generally become close, and for sufficiently large volumes V, the apparent moduli no longer depend on the type of BCs and converge to the effective modulus.

It can be noted that the main differences between the above BCs are related to the handling of (or restrictions for) the fluctuation field $\tilde{\boldsymbol{u}}$ along the boundaries. Therefore, the fluctuation field can be considered the primary factor determining the discrepancy between the solutions obtained with different types of BCs. It is worth noting here that the difference in solutions between the models with the SUBC and OMBC with free lateral boundaries is solely due to the fluctuation field $\tilde{\boldsymbol{u}}$ in uniaxial deformation, thus a comparison between the two using identical model geometries would give quantitative information about the effect of the fluctuation field on the overall solution. Thus, in this study simulations were only performed with the SUBC and OMBC and the results obtained under these two conditions were compared.

Uniaxial tensile simulations were carried out to find the apparent moduli and access the stress and strain fields associated with the two types of BCs just mentioned. For the SUBC, a traction load of 50 MPa was applied on one face of each volume element while the homogeneous deformation $\bar{\boldsymbol{u}}$ on the opposite face along the loading direction was fixed and all the other faces were free of forces. For the OMBC, the same procedures were applied but $\tilde{\boldsymbol{u}} = 0$ was set for all faces so that the volume elements remained orthorhombic during uniaxial deformation.

3. RESULTS AND DISCUSSIONS

3.1. Different strain fields associated with the SUBC and OMBC

Firstly, load-displacement curves were calculated with the SUBC and OMBC assuming plane stress. The next step was to obtain apparent moduli for each volume element using the slope of the load-displacement curves. The apparent moduli obtained with the SUBC and OMBC are plotted as a function of volume element size in Fig. 2. As can be seen in the figure, the moduli obtained with the SUBC and OMBC differ for small volume element sizes, which is perhaps due to the different stress and strain fields associated with the fluctuation field $\tilde{\boldsymbol{u}}$ along their boundaries. The apparent moduli obtained with the SUBC and OMBC converge towards the same value with increasing volume element size, which can be thought of as the effective modulus of the composite microstructure. In most cases, the modulus obtained with the SUBC is lower than for the OMBC, except for $L = 25$, where the moduli obtained by these two conditions are almost identical.

In order to investigate the mechanism that leads to this discrepancy in apparent moduli between the SUBC and OMBC, the difference in strain fields associated with the two BCs was studied in detail. This was done by considering the dif-

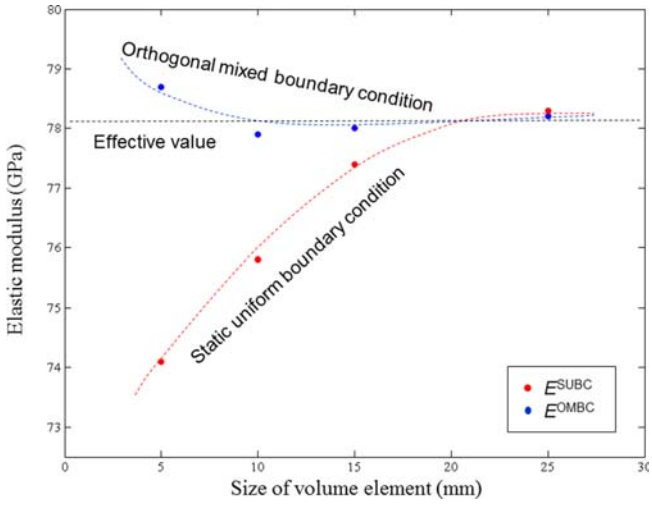

Fig. 2. Apparent elastic moduli obtained with the SUBC and OMBC as a function of the volume element size, showing that the apparent moduli converge to the effective value with increasing sizes. The expected profiles for the two apparent moduli and the effective modulus are also depicted, in dotted lines.

ference between the elastic strains at each node point, as detailed below.

$$\left|\frac{\Delta\varepsilon_{el}(x)}{\boldsymbol{\varepsilon}_{el}^{mean}(x)}\right| = \frac{2\cdot\left|\varepsilon_{el}^{SUBC}(x)-\varepsilon_{el}^{OMBC}(x)\right|}{\left|\varepsilon_{el}^{SUBC}+\varepsilon_{el}^{OMBC}(x)\right|} \tag{9}$$

Here, $\Delta\varepsilon_{el}(x)$ is the difference in elastic strain at node point x, and $\boldsymbol{\varepsilon}_{el}^{SUBC}$ and $\boldsymbol{\varepsilon}_{el}^{OMBC}$ are the strain fields associated with the SUBC and OMBC, respectively. The difference in the strain was normalized with respect to the mean elastic strain, $\boldsymbol{\varepsilon}_{el}^{mean}$.

Figure 3 shows one example of the difference in elastic strain for a volume element with $L = 15$. Clearly, the differences in local strain between the two models are larger near the model boundaries than in the inner part of the model. Since the material parameters, finite element meshes and applied loads were all identical in the models for $\boldsymbol{\varepsilon}_{el}^{SUBC}$ and $\boldsymbol{\varepsilon}_{el}^{OMBC}$, the discrepancies between the two can be thought of as a direct consequence of the deformations associated with $\tilde{\boldsymbol{u}}$ along the model boundaries. Figure 3 also shows enlarged local strain fields associated with the two BCs (Figs. 3(e) and (d)). The deformed boundary in the model with the OMBC was flat due to the restriction of Eq. 5, while that with the SUBC showed significant displacement fluctuations along the boundaries. In the figure, large strain discrepancies between the two models are observed near the free-edges of the particle/matrix interfaces at the boundaries, implying that the fluctuations are mainly associated with model heterogeneities near the boundaries.

3.2. BC-affected region

One interesting point in Fig. 3 is that the change in BCs does not have much effect on the local strain fields in the inner part of the models. This can be seen more clearly in Fig. 4, where the elastic strain differences at all node points are plotted as a function of their distance from the boundaries. As shown in Fig. 4, with increasing distance from the boundary, the discrepancy in strain between the two models tends to decrease very sharply at first, and then stabilizes near zero for distances greater than approximately 2.5 mm (except for $L = 5$, for which the maximum distance was 2.5 mm). With $L = 25$ for instance, more than 90% of node points showed discrepancies less than 1.5% of their mean local strains for distances from the boundaries greater than 2.5 mm. Another interesting numerical aspect is that the thickness of the BC-affected region (where the local stress and strain fields are strongly affected by the particular BCs applied) is almost independent of the size of the volume element. As shown in Fig. 4, the thickness of the BC-affected region was approximately 2.5 mm for all volume element sizes considered in the study.

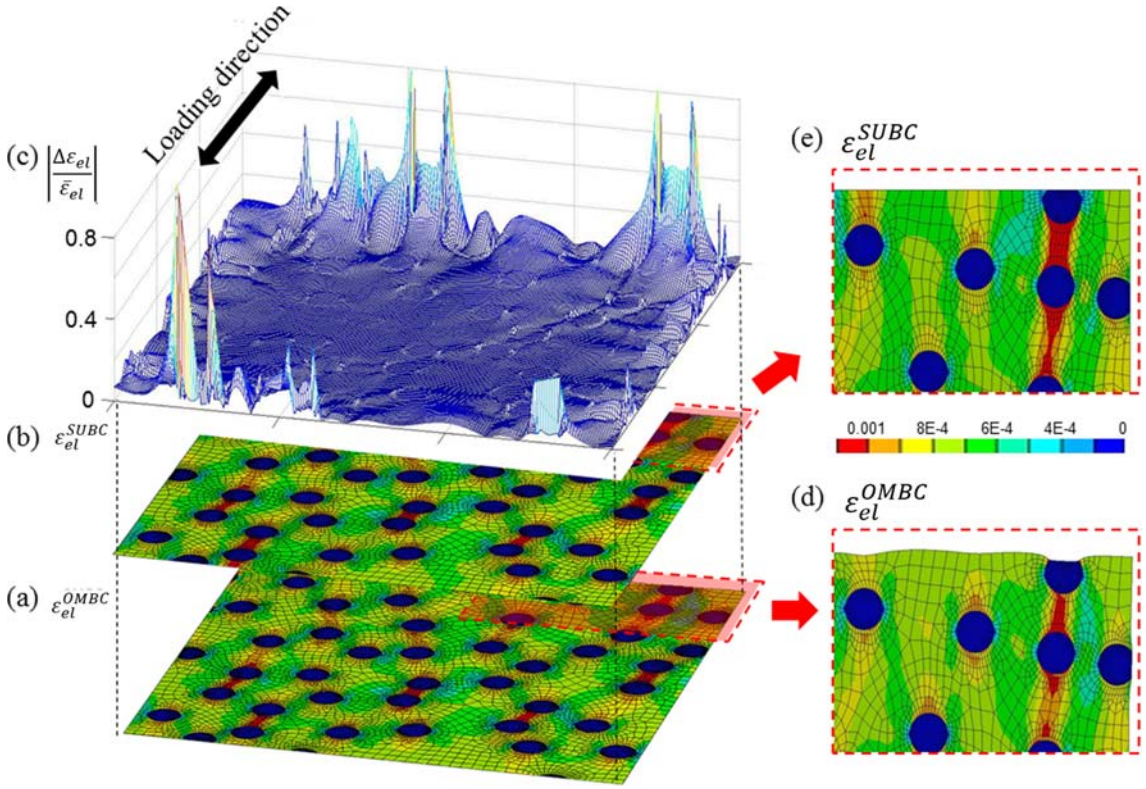

Fig. 3. Elastic strain fields associated with (a) the OMBC and (b) the SUBC. (c) Normalized difference in elastic strain, and (d, e) enlarged contours of the elastic strain fields.

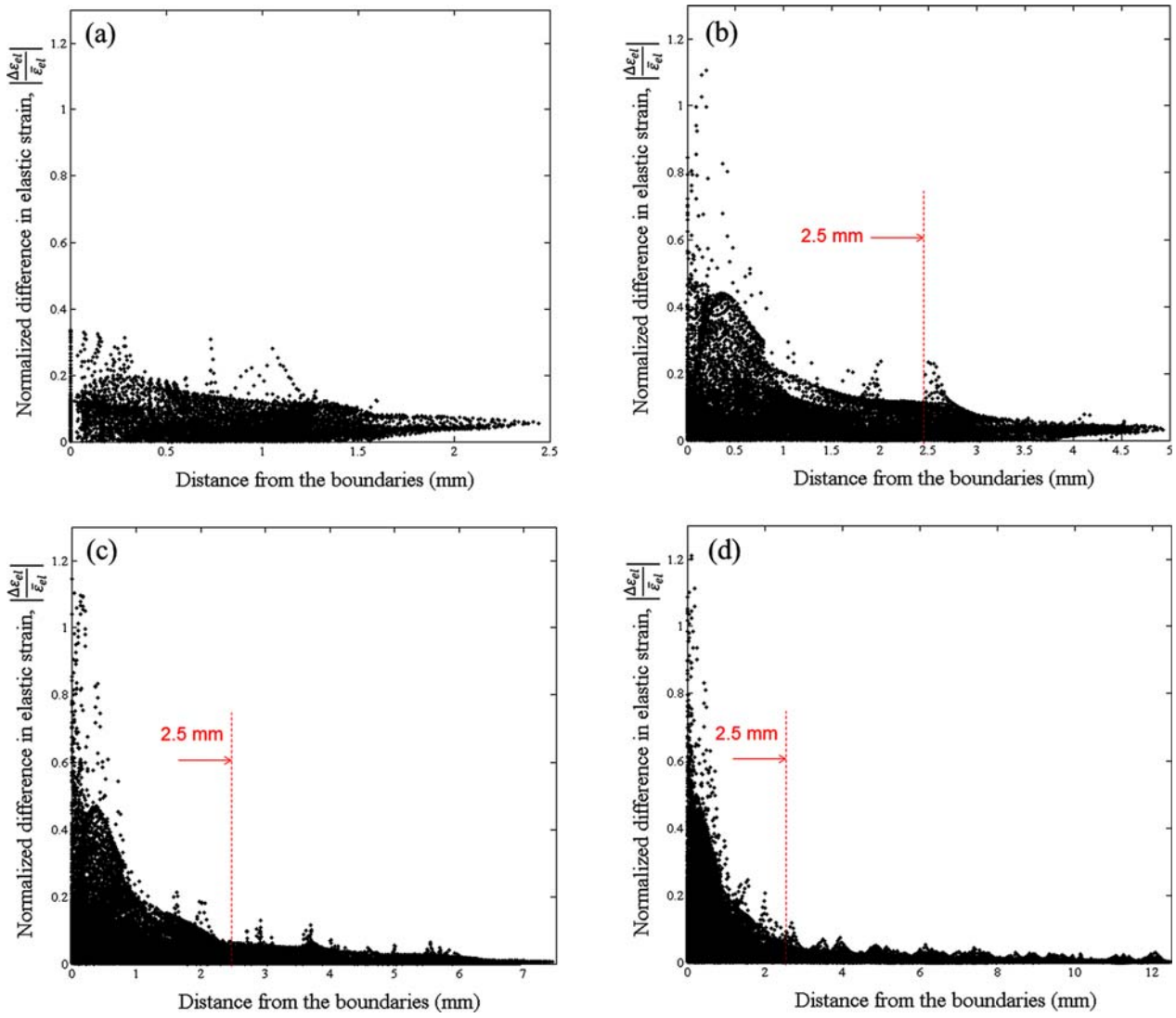

Fig. 4. Normalized differences in elastic strain at all finite element node points as a function of their distance from the boundaries, for volume elements with different side lengths (a) $L = 5$, (b) $L = 10$, (c) $L = 15$, and (d) $L = 25$.

As stated by many researchers [3,18,27], the size of a RVE can be related directly to the convergence of the apparent properties obtained with different types of BCs. Indeed, when a volume element is large enough to be representative of the whole microstructure, its apparent properties are independent of the type of BCs applied. Theoretically therefore, if the volume element V is a RVE, the difference in apparent moduli obtained with the SUBC and OMBC must vanish. When interpreting the present numerical results, this condition may be achieved in practice for linear elastic problems when the volume element is significantly larger than the thickness of the BC-affected region. As shown in Fig. 2, the profiles of the apparent moduli with both the SUBC and OMBC approach the effective modulus nonlinearly with increasing L, with logarithmic-like curvatures. This kind of behavior can also be found in many previous researches (e.g. Refs. [3,29]) and can be understood by considering that the proportion of BC-affected region in the volume elements is inversely related to L by a negative power function (specifically, for a certain thickness t, the proportion of BC-affected region in the total volume varies as $4tL^{-1}$-$4t^2L^{-2}$ in the 2D case), if the thickness of this region from the model boundaries remains the same.

3.3. Effect of the particle volume fraction and the nonlinear material parameter

The effect of the particle volume fraction on the thickness of the BC-affected region was estimated with the models shown in Figs. 1(e) and (f), following the same procedure used in Section 3.2. Figure 5 plots the thickness of the BC-affected region as a function of the particle volume fraction for volume elements with $L = 15$. It clearly shows that the particle volume fraction has significant impact on the thickness of

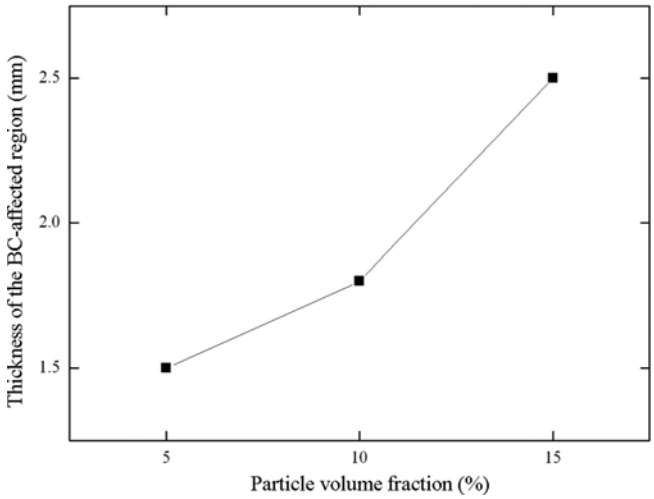

Fig. 5. Effect of the particle volume fraction on the thickness of the BC-affected region for a volume element with a side length $L = 15$.

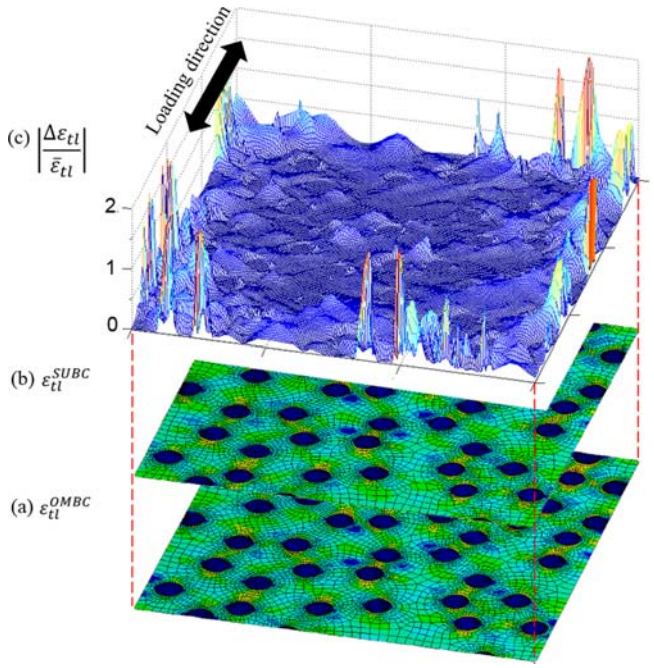

Fig. 6. Total strain field for a model subjected to plastic deformation associated with (a) the OMBC and (b) the SUBC; and (c) the normalized difference in total strain.

the BC-affected region. As the particle volume fraction increases from 5 to 15%, the thickness of the BC affected region increases from 1.5 to 2.5 mm. It seems that the more particles are included in the model, the more heterogeneity is introduced, which can increase the structural fluctuation along the model boundaries. This result suggests that the (absolute) RVE volume should be larger when the model deals with larger particle volume fractions.

Figure 6 shows the differences in total strain ($\varepsilon_{tot} = \varepsilon_{el} + \varepsilon_{pl}$) obtained with different BCs for a RVE with $L = 15$ when the

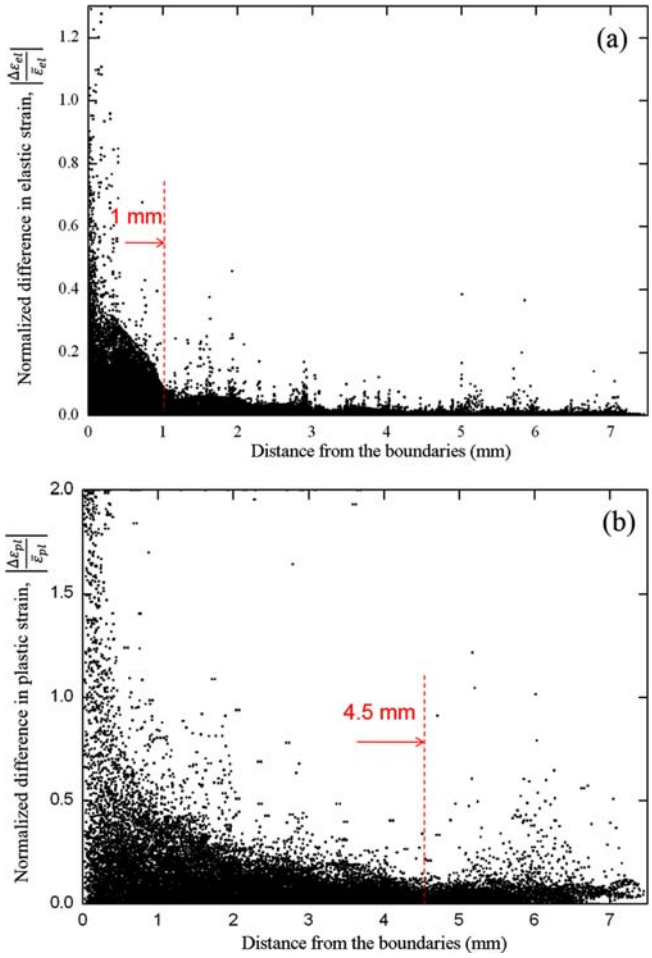

Fig. 7. Normalized differences in (a) elastic strain, (b) plastic strain at all finite element node points when the model is subjected to plastic deformation.

matrix material is subjected to nonlinear elastic-plastic deformation. The tendencies of the results with plasticity and for the pure elastic case are almost identical. As shown in the figure, large differences in the total strain are calculated in the vicinity of the boundaries while in the interior, the total strain estimated with the two different BCs is almost identical. Figures 7(a) and (b) plot the differences between elastic and plastic strains, respectively, at all node points as a function of their distance from the boundaries. Interestingly, Fig. 7(a) shows that the BC-affected region gets thinner from 2.5 mm (for the pure elastic case) to approximately 1 mm when the plasticity of the matrix is introduced. This means that plasticity leads to reduced structural fluctuation, probably because a portion of the applied force turns to plastic deformations in this case. On the other hand, the difference in the plastic strain of the models with the two BCs is more significant compared to the elastic strain of them. Comparing Fig. 7(b) with Fig. 4 clearly shows that both the magnitude of the difference in strain and the thickness of the BC-affected region increase markedly with the introduction of plasticity. Figure

7(b) shows that the thickness of the BC-affected region with plasticity is 4.5 mm when the plastic strain is considered. A larger volume element would therefore be required for numerical simulations with plasticity, in agreement with previous observation by Gitman *et al.* [7], which clearly shows that the variation between RVE models becomes significant when plasticity is considered.

3.4. Discussions

Based on the numerical results and considerations presented in Sections 3.1-3.4, the following mechanism can be proposed through which the apparent properties of RVEs approach the effective ones with increasing the size of *V*. When an external stress is applied to a certain heterogeneous volume element, force and/or displacement fluctuations are produced along the boundaries of the volume, depending on the type of BC used. This fluctuation disturbs the internal stress and strain fields near the boundaries, making the apparent properties of the volume differ from the effective ones. If the thickness of this BC-affected region is independent of the size of the volume element, its proportion in the overall volume decreases logarithmically with increasing volume element size and the apparent properties obtained with different types of BCs approach the effective ones. In this case, a volume element is representative of the whole structure when its size is large enough that the effects of force/displacement fluctuations near the boundaries are negligible. On the other hand, if the BC-affected region spreads into the interior of the element with increasing volume element size, a RVE may not exist and the effective properties cannot be obtained in practical modeling approaches due to the absence of convergence between the apparent properties associated with different types of BCs. With heterogeneity and nonlinearity, the required volume increases since the thickness of the BC-affected region increases, as shown in Section 3.3.

Although this study covers an important fundamental aspect of RVE approaches, several important issues still need to be understood. For instance, this study has been limited to a secondary phase with a fixed shape and size and particle volume fractions below 15%. Another limitation of this study lies in its consideration of only two types of BCs. A detailed study using more complex geometries and various material parameters is required for a better understanding of the interesting phenomena revealed in this study. These investigations are presently underway and will be reported in a later paper.

4. SUMMARY AND OUTLOOK

In the literature several types of BCs have been developed and used for evaluating the homogenized mechanical properties of heterogeneous media with RVE approaches, as shortly introduced in Section 2.2 of this paper. However none of these represent the actual deformation characteristics of volume elements in real materials, since in real materials internal local deformations are non-periodic and highly random. Using the simple numerical test of uniaxial loading in a random particle composite, this paper proposes guidelines for these unrealistic boundary conditions to be used to estimate effective material properties.

The local and overall deformation characteristics of a random composite material were analyzed using models with different volume element sizes and with two types of BCs, the SUBC and OMBC. The main difference between the two BCs lies in the presence of a strain fluctuation field $\tilde{\boldsymbol{u}}$ along the model boundaries in the SUBC, while this is prohibited by the OMBC. Comparisons between the deformed geometries of the models with two different BCs showed that stress or displacement fluctuations developed during deformation along the model boundaries. Interestingly, strain fields associated with the two sets of BCs differed only near the model boundaries, while the inner parts of the models showed almost identical strain fields. It seems that thickness of this BC-affected region is independent of the size of the volume element in the model. For the composites containing 15% spherical particles with a radius of 1 mm considered in this study, the thickness of the BC-affected region remained approximately constant (~2.5 mm) when the size of the model was increased from 5 to 25 mm. With increasing volume element size, the proportion of BC-affected regions in the element decreased and the apparent properties obtained with different types of BCs became close to each other and converged to the effective ones.

The effect of the particle volume fraction was investigated using models with the same size but with different particle contents. The effect of the plasticity of the matrix was also investigated. As the volume fraction of the particles was increased from 5 to 15%, the size of the BC-affected region increased from 1.5 to 2.5 mm. The thickness of the region also increased with plasticity to approximately 4.5 mm. This suggests that with a higher volume fraction of the secondary phase and with nonlinear material deformation, a larger volume has to be considered in the model.

The results of this paper indicate that there are fundamental principles for RVE models to be representative of real microstructures, and these are closely related to the thickness of the BC-affected region in the model. For example, if the thickness is independent of the size of the volume element, RVEs exist in practice because the apparent properties of the volume element will continuously approach the effective ones as the size of the volume element is increased. In contrast, if the BC-affected region spreads into the interior of the volume element as its size is increased, a RVE may not exist and the apparent properties obtained with different types of BCs will remain different even when significantly larger volumes are considered. As such, the mechanism proposed in this paper

can serve as a guide to determining the existence of a RVE for certain research purposes or for quantifying the potentials errors in the apparent properties predicted. These investigations, now under study, would be very useful for estimating the representativity of RVEs, especially for more complicated and nonlinear simulations, for instance of plasticity, fatigue, and creep behaviors.

REFERENCES

1. V. Kouznetsova, W. A. M. Brekelmans, and F. P. T. Baaijens, *Comput. Mech*. **27**, 37 (2001).
2. F. Roters, P. Eisenlohr, L. Hantcherli, D. D. Tjahjanto, T. R. Bieler, and D. Raabe, *Acta Mater.* **58**, 1152 (2010).
3. T. Kanit, S. Forest, I. Galliet, V. Mounoury, and D. Jeulin, *Int. J. Solids Structures* **40**, 3647 (2003).
4. S. Ghosh, K. Lee, and P. Raghavan, *Int. J. Solids Structures*, **38**, 2335 (2001).
5. A. Wongsto and S. Li, *Compos. Part A* **36**, 1246 (2005).
6. D. Trias, J. Costa, A. Turon, and J. E. Hurtado, *Acta Mater.* **54**, 3471 (2006).
7. I. M. Gitman, H. Askes, and L. J. Sluys, *Eng. Fract. Mech*. **74**, 2518 (2007).
8. S. Kari, H. Berger, R. Rodriguez-Ramos, and U. Gabbert, *Compos. Struct.* **77**, 23(2007).
9. H. J. Böhm, A. Eckschlager, and W. Han, *Comput. Mater. Sci*. **25**, 42 (2002).
10. S. K. Paul, *Modelling Simul. Mater. Sci. Eng*. **21**, 055001 (2013).
11. E.-Y. Kim, H. S. Yang, S. H. Han, J. H. Kwak, and S. H. Choi, *Met. Mater. Int*. **18**, 573 (2012).
12. R. Hill, *J. Mech. Phys. Solids* **11**, 357 (1963).
13. Z. Hashin, *J. Appl. Mech*. **50**, 481 (1983).
14. W. J. Drugan and J. R. Willis, *J. Mech. Phys. Solids* **44**, 497 (1996).
15. M. Ostoja-Starzewski, *Prob. Eng. Mech*. **21**, 112 (2006).
16. Y. S. Song and J. R. Youn, *Polymer*. **47**, 1741 (2006).
17. J. Yvonnet, Q. C. He, and C. Toulemonde, *Compos.Sci. Tech.* **68**, 2818 (2008).
18. K. Sab, *Eur. J. Mech. A* **11**, 585(1992).
19. C. Huet, *J. Mech. Phys. Solids*, **38**, 813 (1990).
20. S. Hazanov and C. Huet, *J. Mech. Phys. Solids*, **42**, 813 (1995).
21. B. Widom, *J. Chem. Phys.* **44**, 3888 (1966).
22. W. J. Lee, J. H. Son, N. H. Kang, I. M. Park, and Y. H. Park, *Scripta Mater*. **61**, 580 (2009).
23. W. J. Lee, J. H. Son, I. M. Park, and Y. H. Park, *Comput. Mater. Sci*. **48**, 802 (2010).
24. Y. Nakasone, S. Yoshimoto, and T. A. Stolarski, Engineering Analysis with ANSYS Software, Butterworth-Heinemann, Oxford (2007).
25. S. Hazanov, *Acta Mater.* **134**, 123 (1999).
26. S. Hazanov and M. Amieur, *Int. J. Eng. Sci*. **33**, 1289 (1995).
27. C. Huet, *Mech. Mater.* **31**,787 (1999).
28. Z. F. Khisaeva and M. Ostoja-Starzewski, *J. Elasticity.* **85**, 153 (2006).
29. S. R. Annapragada, D. Sun, and S. V. Garimella, *Comput. Mater. Sci.* **40**, 255 (2007).